

# Synthesis, characterization and luminescence study of dimethyl( $\beta$ -ketoiminato)gallium (-indium) complexes: crystal structure of dimethyl[1-phenyl-3-*N*-(4-methoxyphenylimino)-1-butanonato]gallium

Yingzhong Shen<sup>a,b,1</sup>, Jianlin Han<sup>a</sup>, Hongwei Gu<sup>a</sup>, Yu Zhu<sup>c</sup>, Yi Pan<sup>a,\*</sup>

<sup>a</sup> Department of Chemistry, School of Chemistry and Chemical Engineering, Nanjing University, Nanjing 210093, PR China

<sup>b</sup> Institut für Chemie, Technische Universität Chemnitz, Straße der Nationen 62, 09111 Chemnitz, Germany

<sup>c</sup> Analysis Center of Zhengzhou University, Zhengzhou 450052, PR China

Received 22 December 2003; accepted 11 July 2004

Available online 15 September 2004

## Abstract

Six dimethylgallium (indium) complexes of type  $\text{Me}_2\text{ML}$  [ $\text{M} = \text{Ga}$ ,  $\text{L} = 1\text{-phenyl-3-}N\text{-(phenylimino)-1-butanonato (1)}$ ,  $1\text{-phenyl-3-}N\text{-(}p\text{-methoxyphenylimino)-1-butanonato (2)}$ ,  $1\text{-phenyl-3-}N\text{-(}o\text{-chloro phenylimino)-1-butanonato (3)}$ ;  $\text{M} = \text{In}$ ,  $\text{L} = 1\text{-phenyl-3-}N\text{-(phenyl imino)-1-butanonato (4)}$ ,  $1\text{-phenyl-3-}N\text{-(}p\text{-methoxyphenylimino)-1-butanonato (5)}$ ,  $1\text{-phenyl-3-}N\text{-(}o\text{-chloro phenylimino)-1-butanonato (6)}$ ] have been synthesized by reaction of trimethylgallium (indium) with appropriate 1-phenyl-3-*N*-(arylimino)-1-butanones. The complexes obtained have been characterized by elemental analysis,  $^1\text{H}$  NMR, IR and mass spectroscopy. Structure of **2** has been determined by X-ray single-crystal analysis, in which Ga atom is four coordinated. Complexes **1–6** emit colors from blue to green (463–491 nm) when irradiated by UV light. The electroluminescent (EL) properties of **1–6** were examined by fabricating EL devices using **1–6** as emitter, respectively. The EL bands are located in the green region (509–522 nm).

© 2004 Elsevier B.V. All rights reserved.

**Keywords:** Trimethylgallium; Trimethylindium;  $\beta$ -Ketoimine; X-ray crystallography; Electroluminescence

## 1. Introduction

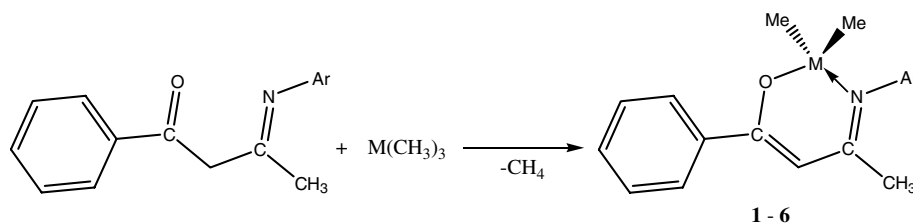
The chemistry of organogallium or indium complexes has attracted much more attention recently because of their interesting applications in chemical reactions [1] and in materials science [2–4]. Organic electroluminescent devices (OLEDs) have been widely studied due to their potential emission of all colors (from blue to red) and their possible applications in large-area displays, since Tang et al. [5,6] reported

the bright OLEDs at low voltages. Most of the reported electroluminescent organic compounds in OLEDs are either aromatic molecules or organic polymers [7–10]. Although quite a few metallic complexes such as 8-hydroxyquinoline or azomethine coordinated Al(III), Zn(II) or Be(II) complexes have been used as OLED emitting material [11–14], few organogallium (indium) compound-based electroluminescent diodes were known up to our knowledge [15,16]. As part of our continuing efforts in searching for new OLEDs light-emitting materials based on organogallium (indium) complexes [3,15,17], we report here the synthesis and characterization of various  $\beta$ -ketoiminato gallium (indium) complexes and their application in electroluminescent devices.

\* Corresponding author. Tel: +86 25 3592485; fax: +86 25 3317761.

E-mail addresses: [yingzhong.shen@chemie.tu-chemnitz.de](mailto:yingzhong.shen@chemie.tu-chemnitz.de) (Y. Shen), [yipan@netra.nju.edu.cn](mailto:yipan@netra.nju.edu.cn) (Y. Pan).

<sup>1</sup> Tel: +49 371 531 1381; fax: +49 371 531 1200.



Scheme 1. Synthesis of complexes 1–6.

## 2. Result and discussion

### 2.1. Synthesis and characterization

Reactions of ketoimine ligands, prepared by condensation of 1-benzoylacetone with aniline, *p*-methoxyaniline and *o*-chloroaniline, respectively, with trimethylgallium (-indium) in 1:1 stoichiometry proceeded smoothly at room temperature affording the corresponding dimethylgallium (-indium) ketoiminato complexes 1–6 (Scheme 1; Table 1).

The complexes (1–6) were isolated as yellow solids in almost quantitative yields. Although trimethylgallium (-indium) is extremely moisture and oxygen sensitive, the complexes obtained, however, are fairly stable on exposure to air. They could be left in ambient atmosphere for months without obvious decomposition. The complexes obtained are sparingly soluble in cold saturated hydrocarbons such as pentane or petroleum and fairly soluble in unsaturated hydrocarbons such as benzene or toluene. All products obtained gave satisfactory elemental analysis results and have been characterized by  $^1\text{H}$  NMR, IR and mass spectroscopy, respectively.

In the  $^1\text{H}$  NMR spectra, the signal of the central methine proton of  $\beta$ -ketoiminato entities in the compounds appears up-field (1: 5.63, 2: 5.61, 3: 5.67, 4: 5.89, 5: 5.86, 6: 5.91 ppm) comparing with the free ligands (6.12 ppm). The chemical shifts of the methine protons for the gallium complexes (1–3) (5.61–5.67 ppm) are slightly smaller than the indium ones (4–6) (5.86–5.91 ppm), indicating that the donor capacities (donor–acceptor interaction) of the respective building blocks are influenced by different metals. In the complexes 2 and 5, which have the electro-repelling meth-

oxyl substituent, the chemical shifts of the methine protons are up-field shifted comparing with those of the others, indicating the remote influence of the substituents on the phenyl ring to the coordination capability of the ligands to the central metals. Chemical shifts of the metal-bonded carbon protons in gallium complexes (1–3) (from  $-0.23$  to  $-0.36$  ppm) move up-field compared with the related metallic alkylide [TMGa:  $-0.10$  ppm], while those of the indium complexes shifted down-field (from  $-0.08$  to  $-0.07$  ppm). In the IR spectra, there were no visible absorptions of O–H stretch vibration comparing with the free ligands, in accordance with the fact that the active hydrogen in the ligands has reacted with the trimethylgallium or indium via keto–enol tautomerism. The azomethine vibration bands of  $\nu(\text{C}=\text{N})$  and  $\nu(\text{C}=\text{C})$  appear in the range of  $1594$ – $1620$  and  $1573$ – $1595\text{ cm}^{-1}$ , respectively, which are somewhat lower than those of free ligands. Lower vibration bands for C=C and C=N bonds may be due to the pseudo aromatic chelating structure in which the  $\pi$ -electrons are somewhat delocalized. These are in agreement with previous result [18].  $\nu(\text{M}–\text{N})$  vibration bands are visible in the range  $470$ – $430\text{ cm}^{-1}$ . In the mass spectra of the gallium complexes,  $\text{M}^+$  peaks for the complexes 2 and 3 were observed. Although  $\text{M}^+$  peak was not observed for 1, the fragment of eliminating one methyl appeared in high intensity. Relative peak intensities of the gallium containing species agree well with the isotopic distribution of gallium atoms [ $^{69}\text{Ga}$  (ca. 60%),  $^{71}\text{Ga}$  (ca. 40%)]. The MS data of indium complexes were not visible in experimental condition because of their difficult gasification.

### 2.2. Solid-state structure of 2

Single crystals of 2 was obtained by recrystallization of a saturated benzene solution containing 2 at  $-20\text{ }^\circ\text{C}$ . The result of the X-ray structure analysis of 2 is depicted in Fig. 1. Crystal data, collection and refinement parameters are summarized in Table 2 and selected bond length ( $\text{\AA}$ ) and angles ( $^\circ$ ) are given in Table 3. Complex 2 crystallizes in the triclinic space group  $P\bar{1}$  (#2). Although quite a few dimethylgallium complexes were found to be dimeric [19–21], compound 2 exists as monomer in solid state. Gallium atom is in distorted

Table 1  
Synthesis of complexes 1–6

Compound number	M	Ar
1	Ga	Phenyl
2	Ga	<i>p</i> -Methoxyphenyl
3	Ga	<i>o</i> -Chlorophenyl
4	In	Phenyl
5	In	<i>p</i> -Methoxyphenyl
6	In	<i>o</i> -Chlorophenyl

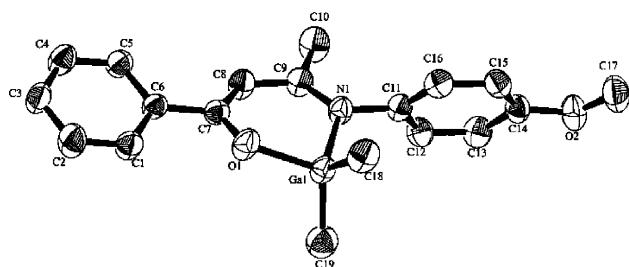


Fig. 1. Molecular structure of **2**, showing 50% probability displacement ellipsoids. Hydrogen atoms are omitted for clarity.

Table 2  
Crystal data, collection parameters, and refinements for **2**

Formula	C <sub>19</sub> H <sub>22</sub> GaNO <sub>2</sub>
Formula weight	366.11
Crystal colour	Yellow
Crystal dimensions (mm)	0.5 × 0.5 × 0.40
Crystal system	Triclinic
Lattice type	Primitive
<i>a</i> (Å)	10.457 (2)
<i>b</i> (Å)	11.176 (8)
<i>c</i> (Å)	9.733 (2)
$\alpha$ (°)	116.40 (2)
$\beta$ (°)	98.38 (3)
$\gamma$ (°)	106.54 (3)
<i>V</i> (Å <sup>3</sup> )	926.3 (8)
Space group	<i>P</i> $\bar{1}$ (#2)
<i>Z</i>	2
<i>D</i> <sub>calc</sub> (g/cm <sup>−3</sup> )	1.313
Index ranges	0 ≤ <i>h</i> ≤ 12, −14 ≤ <i>k</i> ≤ 13, −12 ≤ <i>l</i> ≤ 12
<i>F</i> (000)	380.00
$\mu$ (Mo K $\alpha$ ) (mm <sup>−1</sup> )	1.493
Diffractometer	Rigaku-Raxis IVP
Radiation	Mo K $\alpha$ ( $\lambda$ = 0.71073 Å)
<i>T</i> (K)	288.2
$2\theta_{\max}$ (°)	51.0
Number of reflections measured	2853
Independent reflections observed ( <i>I</i> > 3.00( $\sigma$ ( <i>I</i> )))	2164
Number of variables	209
Correction	Lorentz-polarization
<i>R</i> <sub>1</sub> [ <i>I</i> > 2 $\sigma$ ( <i>I</i> )] <sup>a</sup>	0.0503/0.0701
<i>wR</i> <sub>2</sub> [ <i>I</i> > 2 $\sigma$ ( <i>I</i> )] <sup>b</sup>	0.0702/0.0829
Goodness-of-fit on <i>F</i> <sup>2</sup> <sup>c</sup>	1.24
$\Delta\rho_{\max}$ (e Å <sup>−3</sup> )	0.44
$\Delta\rho_{\min}$ (e Å <sup>−3</sup> )	−0.58
( $\Delta/\sigma$ ) <sub>max</sub>	0.00

<sup>a</sup>  $R_1 = \sum(|F_o| - |F_c|) / \sum |F_o|$ ;

$wR_2 = [\sum(w(F_o^2 - F_c^2)^2) / \sum(wF_o^4)]^{1/2}$ .

<sup>b</sup>  $w = 1/[\sigma^2(F_o^2) + (0.00212P)^2]$ ,  $P = (F_o^2 + 2F_c^2)/3$ .

<sup>c</sup>  $S = [\sum w(F_o^2 - F_c^2)^2 / (n - p)]^{1/2}$ , where *n* is the number of reflections, *p* is the parameters used.

tetrahedron geometry. This may be due to the relatively more crowded environment around gallium bounded O and N atoms. The angle of O–Ga–N is 93.5(2)°, much less than the expected for ideal tetrahedron geometry. The angle of C18–Ga–C19 is 124.3(3)°. These should

Table 3  
Selected bond distances (Å) and angles (°) for **2**

Bond distances			
Ga1–O1	1.930(4)	Ga1–N1	2.009(4)
O1–C7	1.320(6)	N1–C9	1.341(7)
N1–C11	1.451(6)	C7–C8	1.368(7)
C8–C9	1.429(7)	C9–C10	1.509(7)
Bond angles			
O1–Ga1–N1	93.5(2)	O1–Ga1–C18	107.4(2)
O1–Ga1–C19	108.9(2)	N1–Ga1–C18	111.4(2)
N1–Ga1–C19	107.0(2)	C18–Ga1–C19	124.3(3)
Ga1–O1–C7	126.1(3)	Ga1–N1–C9	122.3(3)
Ga1–N1–C11	114.1(3)	O1–C7–C6	114.8(4)
O1–C7–C8	123.0(5)	C6–C7–C8	122.2(5)
C7–C8–C9	129.0(5)	N1–C9–C8	122.8(4)
N1–C9–C10	120.6(5)	C8–C9–C10	116.6(5)
N1–C11–C12	121.9(5)	N1–C11–C16	119.9(4)

demonstrate the rather weak coordination of the nitrogen to the central gallium. The ring GaO1C7C8C9N1 is co-plane, caused by the strain in the ring. The dihedral angle between the plane with the phenyl plane (C1–C6) is 16.58° and the dihedral angle between the plane with the other phenyl plane is 113.11°. O–Ga distance (1.930(4) Å) in the complex is slightly longer than that of dimethyl[*N*-salicylidene 2-aminopyridine] gallium (1.917 Å) [22], the N–Ga distance (2.201(4) Å) which is longer than that of dimethyl[*N*-salicylidene 2-amino-pyridine]gallium (2.059 Å) [22,24].

### 2.3. Photoluminescence studies

Photoluminescence emission spectra (solid) of the complexes **1–6** were measured as shown in Fig. 2. It shows that the emission bands are located in the blue green region (from 463 to 491 nm). When irradiated by UV light, the maximum emission wavelengths are at 463 nm with an intensity of 2.995 a.u. for complex **1**; 491 nm with an intensity of 6.238 a.u. for **2**, 467 nm with an intensity of 2.779 a.u. for **3**, 467 nm with an intensity of 5.197 a.u. for **4**, 468 nm with an intensity of 3.179 a.u. for **5** and 467 nm with an intensity of 2.754 a.u. for **6**. Complexes **2** and **4** exhibit relatively stronger photoluminescence intensities. Stronger photoluminescence intensity and an obvious red-shift of emission bands for the gallium complex **2** comparing to those of **1** and **3** should attribute to the electro-repelling characteristic of the methoxyl group, for **2** which shorten the energy gap between the HOMO and the HOMO levels. Chlorine containing complexes (**3** and **6**), exhibit relative lower photoluminescence intensities, illustrating that chlorine has luminescence quenching effect. Photoluminescence spectra of the compounds **1–6** are in sharp contrast to those of the free ligands. The stronger photoluminescence intensities of the metallic complexes could be attributed to the coordination or bridging of ligand to the metal center, which increases the rigidity

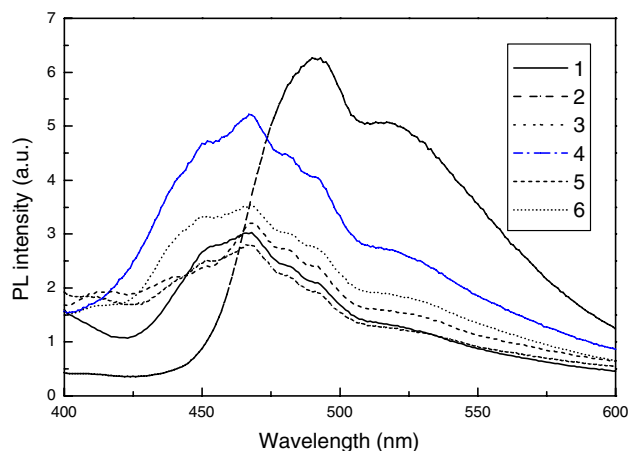


Fig. 2. PL emission spectra of **1–6** in solid state.

of the ligands and reduces the loss of energy via un-radiation pathway, thus enhancing the  $\pi^* \rightarrow \pi$  irradiation probability.

#### 2.4. Electroluminescence studies

The electroluminescence device structure is shown in Fig. 3. The gallium (indium) complexes were used as emitter. The device was prepared on patterned indium–tin-oxide (ITO) coated on glass substrate, which was cleaned by ultrasonic in a mixture of isopropanol and water (1:1) and degassed in toluene vapor, with a sheet resistance of near  $80 \Omega/\square$ . Because the complexes are electro-conducting, hole-injecting material poly(vinylcarbazole) (PVK) was added to improve the balance of current carrier. Due to the poor film-forming properties of the complexes, a very small quantity of poly(methylmethacrylate) (PMMA), which is inert to light and electricity, was used to improve the film-forming properties by mixing it with the organogallium (indium) complexes. A device structure of ITO/emissive layer/Al was employed. High-quality film can be obtained by spin-cast of PMMA, PVK as well as the metallic complexes mixture dissolved in dichloromethane. An electron injecting electrode Al was deposited on top by vacuum evaporation at pressure below  $2 \times 10^{-5}$  Torr with a deposition rate of  $10\text{--}15 \text{ \AA/s}$ . The emitting area was  $2 \times 3 \text{ mm}^2$ . The luminance of the electroluminescent (EL) devices was measured with a Per-

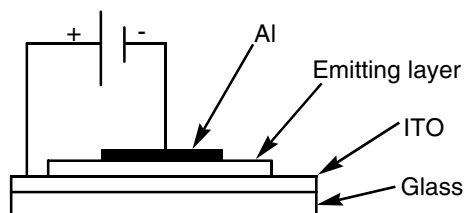


Fig. 3. Configuration of the EL device.

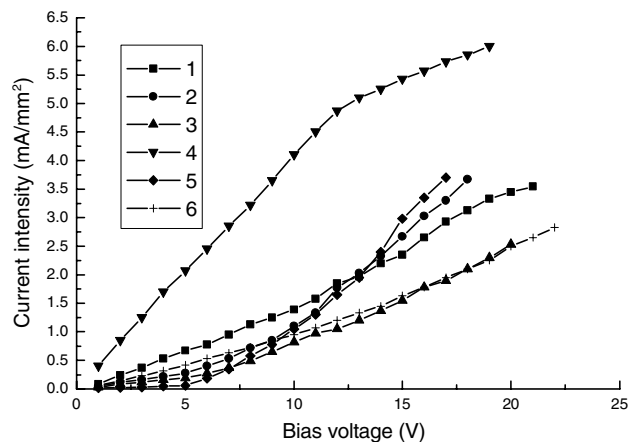


Fig. 4. The relationship between current density and voltage of diodes with the emitter of complexes **1–6**.

kin–Elmer LS 50B fluorescence spectrophotometer. Meanwhile, the current density was recorded with a digital multimeter. All measurements were carried out at room temperature under DC bias conditions.

The current–voltage relationships of the EL devices are shown in Fig. 4. The forward bias current can be obtained when the ITO electrode is positively biased and the Al electrode negatively. Current density increasing rate is proportional to the bias voltage. It increases from  $0.085$  to  $3.55 \text{ mA/mm}^2$  for **1** ( $1\text{--}21 \text{ V}$ ), from  $0.04$  to  $3.67 \text{ mA/mm}^2$  for **2** ( $1\text{--}18 \text{ V}$ ), from  $0.03$  to  $2.53 \text{ mA/mm}^2$  for **3** ( $1\text{--}20 \text{ V}$ ), from  $0.4$  to  $6 \text{ mA/mm}^2$  for **4** ( $1\text{--}19 \text{ V}$ ), from  $0.02$  to  $3.7 \text{ mA/mm}^2$  for **5** ( $1\text{--}17 \text{ V}$ ), from  $0.06$  to  $3.1 \text{ mA/mm}^2$  for **6** ( $1\text{--}24 \text{ V}$ ). The current density increasing rate for complex **4** is larger than those of the other complexes.

The EL emission intensity–voltage relationship has been measured and is shown in Fig. 5. The light output of the EL diodes is proportional to the input voltage in the voltage range of  $11\text{--}21 \text{ V}$  (**1**),  $7\text{--}18 \text{ V}$  (**2**),  $6\text{--}20 \text{ V}$  (**3**),  $12\text{--}24 \text{ V}$  (**4**),  $5\text{--}17 \text{ V}$  (**5**) and  $13\text{--}24 \text{ V}$  (**6**). The emission intensity increases with the increasing of the forward bias voltage. The increasing rate of EL intensity for **5** is much more higher than those of the other complexes. As shown in Fig. 5, complex **5** has higher EL intensity comparing with that of complex **2** despite of theirs having same ligands, implying that the different metals have different effect on electroluminescence. Complex **6** has the lowest EL intensity, illustrating that chlorine has luminescence quenching effect. The driving voltages of the devices are fairly low, especially for **5** ( $5 \text{ V}$ ), much lower than that of tri(1,3-diphenyl-1,3-propanedionio)monophenanthroline Eu(III) ( $25 \text{ V}$ ) [23] and similar to that of tris(8-hydroxyquinolino)aluminum (below  $10 \text{ V}$ ) [6]. Complex **5** should be a promising candidate as light-emitting material for further detailed study.

The EL spectra of the diodes are shown in Fig. 6. Their EL bands are located in the green region. The

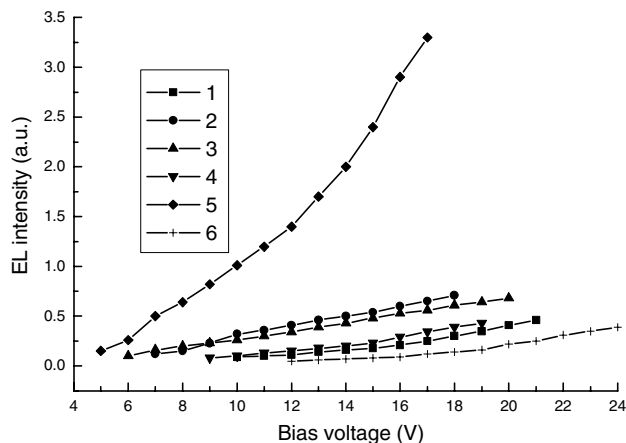


Fig. 5. EL intensity–voltage curve of diodes with the emitter of complexes 1–6.

EL emission maximums are 520 nm with the intensity of 0.18 a.u for **1** (15 V), 522 nm with the intensity of 0.27 a.u for **2** (10 V), 509 nm with the intensity of 0.21 a.u for **3** (10 V), 518 nm with the intensity of 0.10 a.u for **4** (10 V), 520 nm with the intensity of 0.71 a.u for **5** (12 V), 512 nm with the intensity of 0.16 a.u for **6** (19 V). As shown in Fig. 6, the emission bands are similar to those of the PL emission spectra, illustrating that the EL spectra are independent of driving voltage and current. It also indicates that the radioactive recombination of injected electrons and holes takes place in the organometallic complexes. The role of metal atom is considered to be twofold. First, the formation of M–O bond and the donor–acceptor M–N bond changes the  $\pi^* \rightarrow \pi$  transition energy of the ligand. The second, the binding of  $\beta$ -ketoiminato to metal atom increases the rigidity of the ligand, thus reducing the loss of energy via un-radiation vibration motions and increasing the emission efficiency. The maximum EL emitting wavelengths are related to the substituent on the phenyl ring. The maximum emitting wavelength of complexes **3**

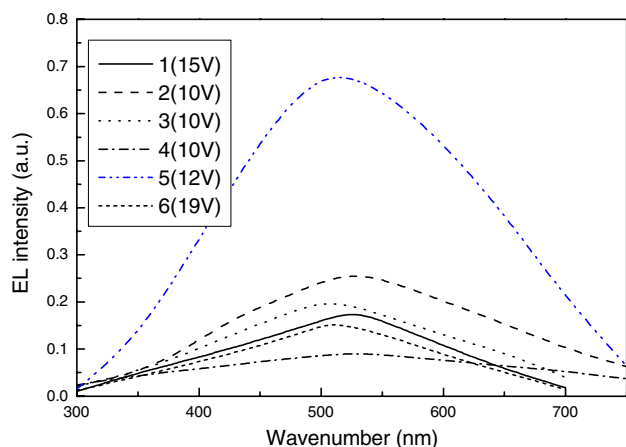


Fig. 6. EL spectra of diodes with the emitter of complexes 1–6.

and **6**, which contain chlorine substituents, shift blueward comparing with other complexes. Maximum EL emitting wavelengths (509–522 nm) shift red-ward comparing with those of PL spectra (463–491 nm). Similar phenomena are observed in the alkylgallium derivatives of thiobenzhydrazones [3].

### 3. Experimental

#### 3.1. General procedure

The solvents were refluxed with sodium benzophenone and distilled under nitrogen prior to use. The ketoimine ligands were prepared by condensation of 1-benzoylacetone with aniline, *p*-methoxyaniline, *o*-chloroaniline. Trimethyl gallium (-indium) were provided by the National 863 Program Advanced Material MO Precursors R&D Center of China. All reactions were performed in a glove box under purified nitrogen. Elemental analysis of C, H, N was performed on a Perkin–Elmer 240C elemental analyzer.  $^1\text{H}$  NMR spectra were recorded on a Bruker ARX-300 spectrometer with TMS as internal standard. Infrared spectra were collected on a Shimadzu IR 408 instrument in KBr pellets. Mass spectra were measured on a VG-ZAB-HS spectrometer (electron impact ionization). Luminescent spectra were measured on Perkin–Elmer LS 50B luminescence spectrometer, melting point was observed in sealed capillaries and were uncorrected.

#### 3.2. Preparation of dimethyl[1-phenyl-3-*N*-(phenylimino)-1-butanonato]gallium (**1**)

Trimethylgallium (1.15 g, 10 mmol), dissolved in 15 mL of cyclohexane, was added dropwise over a period of 10 min with stirring to 1-phenyl-3-*N*-(phenylimino)-1-butanone (2.37 g, 10 mmol), dissolved in 10 mL of cyclohexane and 5 mL of benzene, at room temperature. After stirring the reaction mixture for an additional 30 min at this temperature, all volatiles were removed in oil-pump vacuum and the yellow powder residue was recrystallized from a cyclohexane/benzene solution, giving **1** (2.84 g) in a yield of 84.6% (based on TMGa).

M.p.: 122–124 °C. Anal. Calc. for  $\text{C}_{18}\text{H}_{20}\text{GaNO}$  (336.08): C, 64.33; H, 5.99; N, 4.17. Found: C, 64.03; H, 5.63; N, 4.31%.  $^1\text{H}$  NMR ( $\text{CDCl}_3$ ):  $\delta$  –0.36 (s, 6H, –GaMe<sub>2</sub>), 1.9 (s, 3H, –CH<sub>3</sub>), 5.63 (s, 1H, –CH–), 6.7–7.9 (m, 10H, –ArH). IR data:  $\nu$  ( $\text{cm}^{-1}$ ): 3061 (w), 2959 (w), 1596 (s), 1574 (m), 1509 (vs), 1484 (vs), 1454 (s), 1406 (vs), 1295 (m), 1207 (m), 1113 (m), 952 (w), 852 (m), 761 (s), 707 (vs), 690 (m), 578 (m). MS data: 322.7 (12.92%), 321.8 (68.96%), 320.8 (21.4%), 319.8 (100%), 303.8 (4.13%)

236 (1.16%), 162.8 (6.64%), 160.8 (11.24%), 118 (15.37%), 105 (8.37%), 100.9 (3.18%), 98.9 (3.49%), 77.9 (3.38%), 76.9 (18.06%), 70.8 (12.04%), 68.9 (18.65%).

### 3.3. Preparation of dimethyl[1-phenyl-3-*N*-(*p*-methoxyphenyl imino)-1-butanonato]gallium (**2**)

Prepared as described for **1** from 1-phenyl-3-*N*-(*p*-methoxyphenylimino)-1-butanone (2.67 g, 10 mmol) and trimethylgallium (1.15 g, 10 mmol). Compound was isolated as yellow crystal after recrystallization from benzene. Yield: 3.12 g (85.2%, based on TMGa).

M.p.: 156–158 °C. Anal. Calc. for  $C_{19}H_{22}GaNO_2$  (366.11): C, 62.33; H, 6.06; N, 3.83. Found: C, 61.84; H, 5.89; N, 3.72%.  $^1H$  NMR ( $CDCl_3$ ):  $\delta$  –0.23 (s, 6H, –GaMe<sub>2</sub>), 1.93 (s, 3H, –CH<sub>3</sub>), 3.83 (s, 3H, –OCH<sub>3</sub>), 5.61 (s, 1H, –CH–), 6.8–7.9 (m, 9H, –ArH). IR data:  $\nu$  (cm<sup>–1</sup>): 3050 (w), 2999 (w), 2960 (m), 2931 (w), 2836 (w), 1597 (vs), 1574 (s), 1503 (vs), 1483 (vs), 1406 (vs), 1368 (m), 1295 (s), 1244 (vs), 1208 (m), 680 (m), 582 (m), 567 (m), 544 (m). MS data: 366.9 ( $M^+$ , 0.11%), 365.9 (0.18%), 364.9 (0.32%), 352.9 (13.73%), 351.9 (69.24%), 350.9 (21.94%), 349.9 (100%), 335.8 (5.59%), 333.8 (3.77%), 267 (37.95%), 266 (30.15%), 265 (5.51%), 190.9 (1.49%), 189.9 (6.71%), 162.9 (4.85%), 161.9 (11.38%), 160.8 (5.44%), 148.0 (13.39%), 146.9 (7.96%), 106 (4.03%), 105 (45.28%), 100.9 (3.24%), 98.9 (4.19%), 76.9 (24.32%), 70.8 (6.59%), 68.9 (10.22%).

### 3.4. Preparation of dimethyl[1-phenyl-3-*N*-(*o*-chlorophenyl imino)-1-butanonato]gallium (**3**)

Prepared as described for **1** from 1-phenyl-3-*N*-(*o*-chlorophenylimino)-1-butanone (2.72 g, 10 mmol) and trimethylgallium (2.67 g, 10 mmol). Compound was isolated as yellow crystal after recrystallization from benzene. Yields: 3.07 g (83.1%, based on TMGa).

M.p.: 114–116 °C. Anal. Calc. for  $C_{18}H_{19}NOClGa$  (370.53): C, 58.35; H, 5.17; N, 3.78. Found: C, 58.34; H, 5.08; N, 3.67%.  $^1H$  NMR ( $CDCl_3$ ):  $\delta$  –0.36 (s, 6H, –GaMe<sub>2</sub>), 1.9 (s, 3H, –CH<sub>3</sub>), 5.67 (s, 1H, –CH–), 6.86–7.9 (m, 9H, –ArH). IR data:  $\nu$  (cm<sup>–1</sup>): 3059 (w), 2959 (w), 1594 (s), 1573 (s), 1507 (vs), 1485 (s), 1456 (s), 1405 (vs), 1369 (m), 1295 (m), 1203 (m), 1074 (w), 891 (w), 866 (m), 795 (m), 764 (m), 707 (s), 691 (m), 585 (m). MS data: 370.5 ( $M^+$ , 0.12%), 369.6 (0.19%), 368.5 (0.14%), 358.5 (4.22%), 357.6 (23.1%), 356.6 (19.95%), 355.6 (99.3%), 354.7 (22.55%), 353.7 (100%), 213.7 (1.1%), 117.8 (2.47%), 162.8 (8.89%), 160.8 (13.25%), 151.8 (10.83%), 104.9 (14.39%), 100.9 (4.59%), 76.9 (11.62%), 70.8 (14.72%), 68.8 (22.31%).

### 3.5. Preparation of dimethyl[1-phenyl-3-*N*-(phenylimino)-1-butanonato]indium (**4**)

Prepared as described for **1** from 1-phenyl-3-*N*-(phenylimino)-1-butanone (2.37 g, 10 mmol) and trimethylindium (1.60 g, 10 mmol). Compound was isolated as yellow crystal after recrystallization from benzene. Yield: 3.22 g (84.6%, based on TMIIn).

M.p.: >280 °C (dec.). Anal. Calc. for  $C_{18}H_{20}NOIn$  (381.18): C, 56.72; H, 5.29; N, 3.67. Found: C, 56.53; H, 5.34; N, 3.53.  $^1H$  NMR ( $CDCl_3$ ):  $\delta$  –0.08 (s, 6H, –InMe<sub>2</sub>), 2.14 (s, 3H, –CH<sub>3</sub>), 5.89 (s, 1H, –CH–), 6.9–8.1 (m, 10H, –ArH). IR data:  $\nu$  (cm<sup>–1</sup>): 3057 (w), 2988 (w), 2930 (w), 1612 (s), 1595 (s), 1579 (s), 1548 (m), 1521 (m), 1324 (s), 1284 (m), 752 (m), 689 (m), 518 (m).

### 3.6. Preparation of dimethyl[1-phenyl-3-*N*-(*p*-methoxyphenyl imino)-1-butanonato]indium (**5**)

Prepared as described for **1** from 1-phenyl-3-*N*-(*p*-methoxyphenylimino)-1-butanone (2.67 g, 10 mmol) and trimethylindium (1.60 g, 10 mmol). Compound was isolated as yellow crystal after recrystallization from benzene. Yield: 3.55 g (86.3%, based on TMIIn).

M.p.: >280 °C (dec.). Anal. Calc. for  $C_{19}H_{22}NO_2In$  (411.21): C, 55.49; H, 5.39; N, 3.41. Found: C, 55.31; H, 5.12; N, 3.34%.  $^1H$  NMR ( $CDCl_3$ ):  $\delta$  0.07 (s, 6H, –InMe<sub>2</sub>), 1.98 (s, 3H, –CH<sub>3</sub>), 3.91 (s, 3H, –OCH<sub>3</sub>), 5.86 (s, 1H, –CH–), 6.6–7.92 (m, 9H, –ArH). IR data:  $\nu$  (cm<sup>–1</sup>): 3051 (w), 2992 (w), 2931 (w), 2836 (w), 1597 (vs), 1578 (vs), 1550 (s), 1509 (s), 1442 (m), 1378 (m), 1329 (m), 1249 (s), 1179 (m), 1036 (m), 838 (w), 717 (m), 689 (s), 677 (s), 518 (m).

### 3.7. Preparation of dimethyl[1-phenyl-3-*N*-(*o*-chlorophenyl imino)-1-butanonato]indium (**6**)

Prepared as described for **1** from 1-phenyl-3-*N*-(*o*-chlorophenylimino)-1-butanone (2.72 g, 10 mmol) and trimethylindium (1.60 g, 10 mmol). Complex was isolated as yellow crystal after recrystallization from benzene. Yields: 3.48 g (83.7%, based on TMIIn).

M.p.: 290–292 °C. Anal. Calc. for  $C_{18}H_{19}NOClIn$  (415.63): C, 52.02; H, 4.61; N, 3.37. Found: C, 51.83; H, 4.87; N, 3.65.  $^1H$  NMR ( $CDCl_3$ ):  $\delta$  0.07 (s, 6H, –InMe<sub>2</sub>), 2.16 (s, 3H, –CH<sub>3</sub>), 5.91 (s, 1H, –CH–), 6.7–7.9 (m, 9H, –ArH). IR data:  $\nu$  (cm<sup>–1</sup>): 3053 (w), 2962 (w), 2931 (w), 1620 (s), 1591 (vs), 1571 (s), 1552 (s), 1514 (m), 1438 (m), 1323 (s), 1268 (m), 1262 (m), 1094 (m), 1029 (m), 864 (m), 757 (m), 707 (m).

### 3.8. Crystal structure determination of compound **2**

Single crystal of compound **2** was obtained by recrystallization from benzene solution. A single crystal suitable for X-ray determination was mounted in a

thin-walled capillary tube in a glove box, plugged with resin then flame sealed. Data were collected at 288 K on a Rigaku-Raxis IVP imaging plate area detector with graphite monochromated Mo K $\alpha$  ( $\lambda = 0.71073$  Å) radiation to a maximum  $2\theta$  value  $51.0^\circ$ . Read out was performed in the 0.100 mm pixel mode. A total of 2853 reflections were collected, the intensity data were corrected for Lorentz-polarization factors as well as for absorption. The structure was solved by direct methods [24] expanded using Fourier technique [25]. All non-hydrogen atoms were refined anisotropically. Hydrogen atoms were included but not refined. All calculations were performed using the TEXSAN crystallographic software package of Molecular Structure Corporation [26].

#### 4. Supplementary material

Crystallographic data (comprising hydrogen atom coordinates, thermal parameters and full tables of bond lengths and angles) for the structural analysis has been deposited with the Cambridge Crystallographic Center (Deposition No. CCDC 227130). Copies of this information may be obtained free of charge from The Director, CCDC, 12 Union Road, Cambridge, CB2 1EZ, UK (fax: +44 1223 336033; e-mail: deposit@ccdc.cam.ac.uk or www: <http://www.ccdc.cam.ac.uk>).

#### Acknowledgements

We gratefully acknowledge the National Natural Science Foundation of China, Science Foundation of Jiangsu Province and the 863 High Technology Program for their financial support. The research funds for Y. Pan from Qing-Lan Program of Jiangsu Province and Kua-Shi-Ji Program of Education Ministry of China are also acknowledged.

#### References

- [1] D.A. Atwood, M.J. Harvey, Chem. Rev. 101 (2001) 37.
- [2] J. Ashenhurst, L. Bracaleon, A. Hassan, W. Liu, H. Schmider, S.N. Wang, Q.G. Wu, Organometallics 17 (1998) 3186.
- [3] Y.Z. Shen, H.W. Gu, W.J. Gu, F. Yuan, Y. Zhu, Y. Pan, J. Organomet. Chem. 681 (2003) 51.
- [4] E. Toshio, T. Michiko, O. Satoshi, Eur. Pat. No. 757088, 1997.
- [5] C.W. Tang, S.A. VanSlyke, Appl. Phys. Lett. 51 (1987) 913.
- [6] C.W. Tang, S.A. VanSlyke, C.H. Chen, J. Appl. Phys. 65 (1989) 3610.
- [7] H.J. Brouwer, V.V. Krasnikov, A. Hilberer, G. Hadziioannou, Adv. Mater. 8 (1996) 935.
- [8] Edwards, S. Blumstengel, I. Sokolik, R. Dorsinville, H. Yun, K. Kwei, Y. Okamoto, Appl. Phys. Lett. 70 (1997) 298.
- [9] Y. Ohmori, M. Uchida, K. Muro, K. Yoshino, Jpn. J. Appl. Phys. 30 (1991) L1941.
- [10] J.H. Burroughes, D.D.C. Bradley, A.R. Brown, R.N. Marks, K. Mackay, R.H. Friend, P.L. Burus, A.B. Holmese, Nature 347 (1990) 539.
- [11] T. Sano, M. Fujita, T. Fujii, Y. Nishio, Y. Hamada, K. Shibata, K. Kuroki, US Pat. No. 5432014, 1995.
- [12] Y. Hironaka, H. Nakamura, T. Kusumoto, US Pat. No. 5466392, 1995.
- [13] Y. Hamada, T. Sano, M. Fujita, T. Fujii, Y. Nishio, K. Shibata, Chem. Lett. (1993) 905.
- [14] N. Nakamura, S. Wakabayashi, K. Miyairi, T. Fujii, Chem. Lett. (1994) 1741.
- [15] C.X. Xu, Y.P. Cui, Y.Z. Shen, H.W. Gu, Y. Pan, Y.K. Li, Appl. Phys. Lett. 75 (1999) 1827.
- [16] L.S. Sapochak, A. Padmaperuma, N. Washton, F. Endrino, G.T. Schmett, J. Marshall, D. Fogarty, P.E. Burrows, S.R. Forrest, J. Am. Chem. Soc. 123 (2001) 6300.
- [17] C. Xu, Y. Shen, Y. Li, Y. Cui, Appl. Phys. A 70 (4) (2000) 391.
- [18] S.A. Samath, N. Raman, K. Jeyasubramanian, S.K. Ramalingam, Polyhedron 10 (1991) 1687.
- [19] H. Schumann, M. Frick, B. Heymer, F. Girgsdies, J. Organomet. Chem. 512 (1996) 117.
- [20] R.H. Mauch, K.O. Velthaus, B. Hüttel, U. Troppenz, R. Herrmann, SID 95 Digest (1995) 720.
- [21] Y. Yang, Mater. Res. Soc. Bull. 22 (6) (1997) 31.
- [22] Y.Z. Shen, Y. Pan, H.W. Gu, G. Dong, X.Y. Huang, H.W. Hu, J. Organomet. Chem. 605 (2000) 234.
- [23] D.G. Ma, D.K. Wang, Z.Y. Hong, X.J. Zhao, X.B.J.F.S. Wang, Chin. J. Chem. 16 (1) (1998) 1.
- [24] A. Altomare, M.C. Burla, M. Camalli, M. Cascarano, C. Giacovazzo, A. Guagliardi, G. Polidori, J. Appl. Crystallogr. 27 (1994) 435.
- [25] P.T. Beurskens, G. Admiraal, G. Beurskens, W.P. Bosman, R. de Gelder, R. Israel, J.M.M. Smiths, The DIRDIF-94 Program System, Technical Report of the Crystallography Laboratory, University of Nijmegen, The Netherlands.
- [26] Crystal Structure Analysis Package, Molecular Structure Corporation (1985 and 1992).